Bismuth doping on CuGaS$_2$ thin films: structural and optical properties

Marcos A. S. Andrade Jr. and **Lucia H. Mascaro,** Department of Chemistry, Federal University of São Carlos, Rod. Washington Luiz, Km 235, CEP 13565-905, São Carlos-SP, Brazil

Address all correspondence to Marcos A. S. Andrade at **marcos_asaj@hotmail.com**

Abstract

In this work, we present a solvothermal method to prepare bismuth (Bi)-doped CuGaS$_2$ chalcopyrite nanocrystals ink and apply it to an all-solution-processed approach for the preparation of films with a thickness of approximately 730 nm and with enhanced optical properties and lower band gap energy than the undoped semiconductor films. The low-cost deposition method is comprised by spray deposition of the chalcogenide nanocrystals ink onto the molybdenum substrates, producing microcrystalline films with grains larger than 400 nm originated from coalescence of Bi-doped nanocrystals. Bi-doped CuGaS$_2$ microcrystalline films are a good candidate to be applied as an absorber layer in thin-film solar cells.

Introduction

Thin films solar cells based on chalcopyrite Cu(In,Ga)Se$_2$ (CIGS, $\eta\sim21\%$) are great competitors to achieve the high-energy conversion efficiency of silicon devices ($\eta\sim26\%$ for a crystalline cell).[1, 2] These copper-based ternary chalcogenides are among the promising materials to be applied as absorber layers in solar cells due to their low band gap,[3] high absorptivity coefficient into the visible and next infrared (IR) ranges,[4] high tolerance to defects and impurities and have been extensively studied during the last three decades.[5,6] However, efforts have been made about to seek new absorber materials to allow economical and scalable commercialization of chalcopyrite-based devices.

CuGaS$_2$ is a wide band gap (2.40 eV) ternary chalcogenide,[7] isostructural to the CIGS and has relatively low toxicity.[8] The CuGaS$_2$ is composed by elements more abundant than that chalcogenides based on In, Cd, Se, and Te: for example, (160 ppb) e Ga (16.9 ppm) e Se (0.05 ppm).[9] However, the optimal band gap energy of a single band gap device was calculated to be approximately 1.4 eV according to the Shockley–Queisser limit. Although CuGaS$_2$ has not suitable band gap to act as a light absorption layer in single junction solar cells, it is possible to modulate its band gap by intermediate band formation or lowering the band gap by metal doping. Experimental and theoretical studies have reported an increased optical absorption intensity of CuGaS$_2$ doped with transition metals (Ti,[10] Cr,[11] Ce,[12] and Fe[13]), post-transition (Sn[14]), and 15 group elements (N, P, As, Sb),[7] in comparison with the undoped semiconductor.

The preparation of CuGaS$_2$ thin films have been reported by several physical methods, for example, EBPVD (electron beam physical vapor deposition)[15] and MVPD (metalorganic vapor phase deposition),[16] and spray pyrolysis.[17] These methods are relatively expensive due to the use of vacuum equipment and may present throughput limitations.

In this work, we present a solvothermal method to prepare bismuth (Bi)-doped CuGaS$_2$ nanocrystals ink and we apply it to an all-solution-processed approach for the preparation of microcrystalline films with enhanced optical properties in comparison with the undoped semiconductor films. The low-cost deposition method is comprised by spray deposition of the chalcogenide nanocrystals ink onto the molybdenum (Mo) substrates. Besides, we also discuss the structure, composition, and optical properties of the metal-doped CuGaS$_2$ films.

Experimental

Mo foil (0.1 mm, Sigma-Aldrich) was used as a substrate for all samples in this study. CuGaS$_2$ and Bi-doped nanocrystals were prepared according to Chang et al.[18] Briefly, to prepare Bi-doped chalcopyrite, CuCl (Sigma-Aldrich), Ga$_2$(SO$_4$)$_3$.(Sigma-Aldrich), and Bi(NO$_3$)$_3$ (Sigma-Aldrich) (1:1:0.01, molar ratio Cu:Ga:Bi) were added to a three-neck flask containing oleylamine (Sigma-Aldrich). The mixture was heated up to 240 °C under vigorous stirring. Then, the reaction was started by the immediate injection of the solution of sulfur powder (Acros) in oleylamine, kept under stirring for 1 h, and allowed to cool to room temperature, afterward. The nanocrystals were washed, centrifuged, and redispersed in hexane.

Films were deposited by spraying the nanocrystals hexane solution (0.012 mg/mL) for 2 s on preheated 0.5×1.0 mm^2 Mo foil substrates on a hotplate at 80 °C, and then it was repeated for 20 times, with intervals of 1 min for remaining solvent evaporation. Afterward, the films were annealed at 350 °C for 15 min to remove surfactant and remaining solvent, and at

500 °C for 1 h for improving crystallization under sulfur and nitrogen atmosphere to prevent decomposition of the material.

The composition and morphologies of the nanocrystals precursors and the $CuGaS_2$ and Bi-doped $CuGaS_2$ films were investigated by an EDAX (energy-dispersive x-ray analysis) and field-emission scanning electron microscopy (SEM-FEG, INSPECT F50) techniques. The organization at long distance of the chalcogenides was identified by x-ray diffraction (XRD) analysis performed with Cu K_α radiation (40 kV, 30 mA) using a Shimadzu model XRD 6000 diffractometer. The optical properties of the films were investigated by the UV–vis analysis measured between 300 and 2000 nm on a Cary 5 G Varian UV–vis–near-IR (NIR) spectrophotometer. X-ray photoelectron spectroscopy (XPS) measurements were performed on a Thermo Scientific K-Alpha spectrometer using monochromatic Al K_α (1486.6 eV) radiation.

Results and discussion
Bi-doped $CuGaS_2$ nanocrystals
The ternary chalcogenides nanocrystals were prepared to be applied as building blocking to fabricate thin films using an all-solution processed method of deposition and avoid expensive techniques of vacuum.

The x-ray diffractograms of the nanocrystals [Fig. 1(A)] show the main three peaks (112), (220)/(204), and (312) about 29, 48, and 57° 2θ,[18] respectively, which correspond to the tetragonal chalcopyrite structure reported to $CuGaS_2$ (JCPDS: 75-0103), with space group $I\bar{4}2d$.[7] The broad peaks are characteristics of the nanometer-sized crystals of approximately 15 nm [Fig. 1(B)]. The peak (112) in Bi-doped $CuGaS_2$ diffractogram shifts approximately 1° to lower 2θ degree in comparison with that for $CuGaS_2$, which means that the incorporation of bismuth (Bi) into the chalcopyrite lattice promotes an increase of 0.3 Å in this interplanar distance. It may result from the that Bi atomic "radius" (1.48 Å)
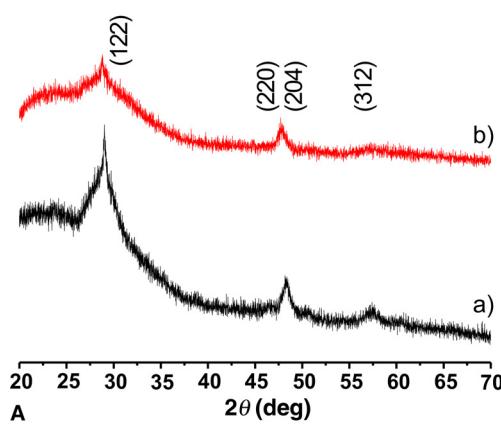
larger than that for Ga (1.22 Å).[19] Once identified the obtaining of Bi-doped $CuGaS_2$ chalcopyrite nanocrystals, they were used fabricate thin films.

The effect of Bi-doped $CuGaS_2$ on the structure and optical properties of thin films
Figure 2 illustrates the procedure employed in this work to prepare microcrystalline thin films using nanocrystals as precursors. As already mentioned above in the experimental part, the $CuGaS_2$ and Bi-doped $CuGaS_2$ nanocrystals solution inks are spray-deposited on Mo foil, followed by annealing at 500 °C under sulfur atmosphere.

An approximation of the stoichiometry of $CuGaS_2$ and Bi-doped $CuGaS_2$ films were determined by the energy-dispersive spectroscopy, presenting the atomic ratio equal to 1:1.02:2.13, and 1:0.96:0.04:2.10, respectively. It suggests that the composition of the Bi-doped material is $CuGa_{0.96}Bi_{0.04}S_{2.10}$, which is in agreement with the expected result.

Figure 2 also shows the top view and cross-sectional SEM images of the films after annealing. As observed, the film of $CuGaS_2$ shows a surface formed by a packing of dense nanoparticles. On the other side, the films fabricated from Bi-doped $CuGaS_2$ solution reveal a film comprised of notable grain growth, with particles size measuring from hundreds nanometer even up to approximate microns. Large grain-based films would decrease the density of deleterious grain boundaries in the direction of transport and enhance charge collection, in addition, the grain size is a parameter that determines series resistance, as well as, it would give higher conversion efficiency for solar cell applications.[20] Bi-doped $CuGaS_2$ crystalline film formed by larger grains present some cracks which can be attributed to a rapid solvent evaporation and during burning the long-chain surfactant.

Figure 3(A) shows the diffractograms of the films prepared by spray deposition of nanocrystalline $CuGaS_2$ and Bi-doped


Figure 1. X-ray diffractograms of (A)—(a) $CuGaS_2$ and (b) Bi-doped $CuGaS_2$ nanocrystals, (B) Image of transmission electron microscopy (TEM) of Bi-doped nanocrystals, and a histogram of the distribution of particle size inset.
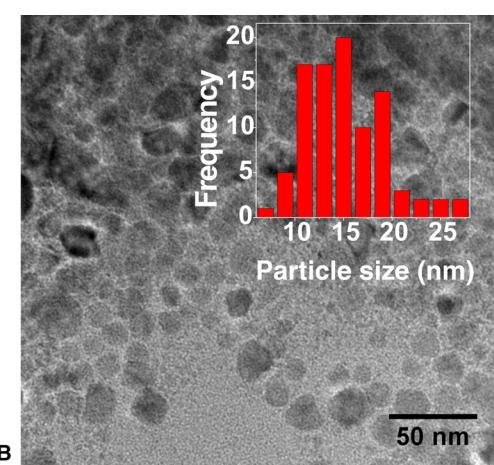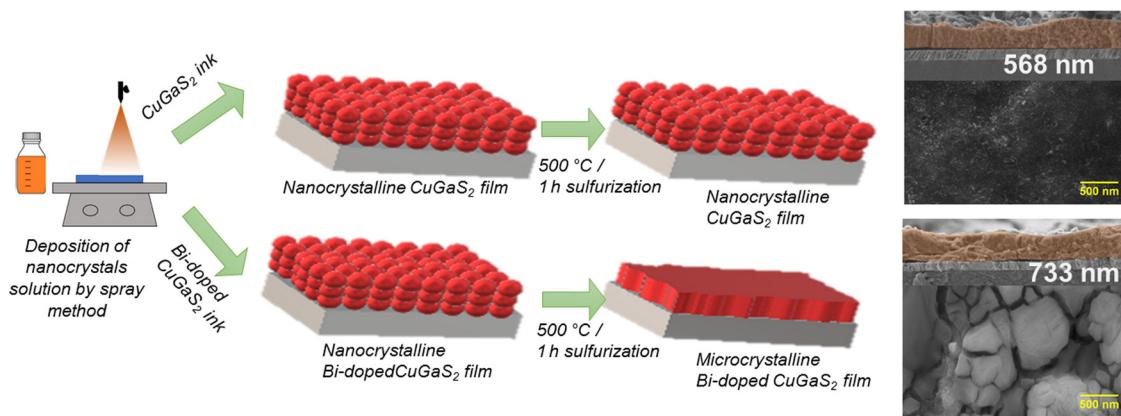
Figure 2. Scheme of microcrystalline bismuth-doped chalcopyrite thin-film preparation, and top view and cross-sectional SEM micrographs of $CuGaS_2$ and Bi-doped $CuGaS_2$ films.

$CuGaS_2$ inks. The diffractograms show two peaks at 41° and 59° 2θ attributed to the Mo substrates,[21] and the main three peaks corresponding to the chalcopyrite structure. There are no peaks related to $CuBi_xS_y$, Cu_xS, or Ga_xS phases in the diffractograms confirming the purity of the films.

The peaks attributed to $CuGaS_2$ [Figs. 3(A, a)] are broader than those peaks in the diffractogram of Bi-doped $CuGaS_2$ [Figs. 3(A, b)], which indicates that the Bi-$CuGaS_2$ films are more crystalline than that undoped film. The crystallite size and growth were calculated using the Debye–Scherrer equation
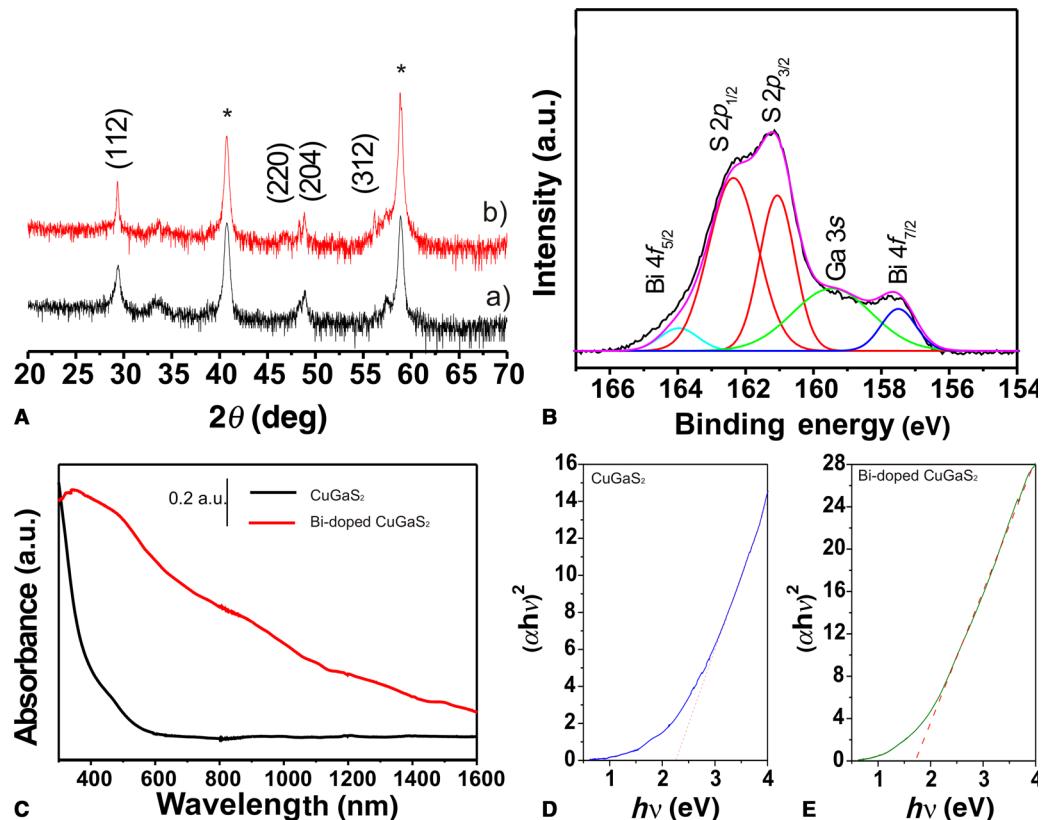
Figure 3. (A) X-ray diffractograms of the (a) $CuGaS_2$ and (b) Bi-doped $CuGaS_2$ films after sulfurization treatment at 500 °C, the peaks signed with * are attributed to Mo substrate. (B) X-ray photoelectron core-level spectrum for S $2p$, Ga $3s$, and Bi $4f$, in Bi-doped $CuGaS_2$ nanocrystals. (C) UV–vis–NIR spectra of the semiconductors. Panels (D) and (E) show the Tauc plots of $CuGaS_2$ and Bi-doped $CuGaS_2$ thin films.

using the FWHM (full-width at half-maximum) of the (112) peak.[22] The diameter of the $CuGaS_2$ nanocrystals was evaluated to be about 20 nm, and to Bi-doped $CuGaS_2$ the diameters were estimated at approximately 500 nm. This result proves the coalescence of the precursors Bismuth-based nanocrystals into large grains.

In literature, it is reported many strategies to use grain growth promoters, such as Sb, Bi, and Mg, to obtain films with large crystallites originated from the coalescence of nanocrystals into large micro-sized grains during annealing. In the work reported by Guijarro et al.[20] is reported the use of a solution of $BiCl_3$ sprayed on the surface of $CuGaS_2$, $CuInS_2$, and $CuGaInS_2$ films to promote the grain growth of the chalcopyrite particles. Although a little is known about the grain growth mechanism, it is already confirmed that microcrystalline metal-doped $CuGaS_2$ films present significant enhancement in the carrier transport and collection of carriers. However, in this current work, we present a direct approach to deposit Bi-doped nanoparticles on the substrate, without further experimental step to metal doping the chalcogenide film. In addition, we ensure the distribution of Bi doping along all the film.

The incorporation of Bi into the chalcopyrite is confirmed by x-ray photoelectronic spectroscopy. Figure 3(B) shows a deconvoluted spectrum containing two peaks at 158.0 and 164.5 eV assigned to Bi $4f_{7/2}$ and Bi $4f_{5/2}$ in Bi-doped $CuGaS_2$.[23] Additionally, the XPS spectrum shows the peaks attributed to S $2p_{1/2}$ and S $2p_{3/2}$ centered at 163 and 161.3 eV, attributed to the different binding with Ga and Cu, respectively, and a peak at 159 eV related to Ga $3s$.[24]

Optical properties of $CuGaS_2$ and Bi-doped $CuGaS_2$ nanocrystals were analyzed using UV–vis–NIR spectroscopy. Figure 3(C) shows that the Bi-doped semiconductor film absorbs stronger in the visible and next IR region than the $CuGaS_2$ nanocrystalline film. From the analysis of the Tauc plots [Figs. 3(D) and 3(E)], the values of the direct band gap of the chalcogenides are estimated in 2.3 eV to $CuGaS_2$ and 1.7 eV to Bi-doped $CuGaS_2$. The optical band gap of $CuGaS_2$ prepared in this work coincides well with those typical tetragonal chalcopyrite reported in the literature, which is between 2.3 and 2.5 eV.[25,26] The E_g of Bi-doped film results in absorption at a wide range of the visible light spectrum and can increase the photon harvesting.[26] Similar results have been reported by Ti, V,[27] Cr,[28] Ni,[29] and Fe[30] doping in chalcogenides. However, specifically considering to $CuGaS_2$, there are several reports on Ti and Cr doping. Jing et al.[8] have shown the effect of the incorporation of Ti on the optical band gap of $CuGaS_2$. The E_g of Ti-doped $CuGaS_2$ films reduced from 2.3 and 1.92 eV with increasing Ti concentrations. The incorporation of 2% of Cr into the mentioned chalcopyrite was reported by Chen et al.[11] The Cr doping resulted in a 1.85 eV band gap. Based on that, Bi doping has a more positive effect on the optical properties of the chalcogenide than the Ti and Cr, and its E_g (1.7 eV) is closer to that optimal band gap energy of a single band gap device according to the Shockley–Queisser limit. According to the literature, the

incorporation of metals in $CuGaS_2$ would generate an intermediate band or decrease the band gap energy which can enhance absorption photons and allow these materials to be applied as a promising absorber layer in chalcogenides thin-film solar cells.[7,29]

Conclusions

Bi-doped $CuGaS_2$ chalcopyrite was synthesized via a simple solvothermal method producing 15.0 nm nanocrystals. The solution of these nanoparticles in hexane result in an ink which was deposited by spray onto Mo substrates. The Bi doping into $CuGaS_2$ promoted a decreased band gap in comparison with the undoped chalcopyrite, broadening the spectral response and improving the light absorption in visible range. Moreover, the incorporation of Bi on $CuGaS_2$ structure promoted grain growth producing microcrystalline films with particles of approximately 400 nm. The ability to improve growth control and quality of the grain structures, and the enhancement in the optical properties highlights Bi-doped $CuGaS_2$ to be applied as an absorber layer in thin-film chalcogenides solar cells.

References

1. T.M. Friedlmeier, P. Jackson, A. Bauer, D. Hariskos, O. Kiowski, R. Menner, R. Wuerz, and M. Powalla: High-efficiency Cu(In,Ga)Se$_2$ solar cells. *Thin Solid Films* **633**, 13 (2016).
2. J. van Deelen, and C. Frijters: CIGS cells with metallized front contact: longer cells and higher efficiency. *Sol. Energy* **143**, 93 (2017).
3. Z. Lu, R. Jin, Y. Liu, L. Guo, X. Liu, J. Liu, K. Cheng, and Z. Du: Optimization of chemical bath deposited cadmium sulfide buffer layer for high-efficient CIGS thin film solar cells. *Mater. Lett.* **204**, 53 (2017).
4. L. Yu, R.S. Kokenyesi, D.A. Keszler, and A. Zunger: Inverse design of high absorption thin-film photovoltaic materials. *Adv. Energy Mater.* **3**, 43 (2013).
5. J. Ramanujam, and U.P. Singh: Copper indium gallium selenide based solar cells – review. *Energy Environ. Sci.* **10**, 1306 (2017).
6. T.D. Lee, and A.U. Ebong: a review of thin film solar cell technologies and challenges. *Renew. Sustain. Energy Rev.* **70**, 1286 (2017).
7. M. Han, X. Zhang, Y. Zhang, and Z. Zeng: The group VA element non-compensated n–p codoping in CuGaS$_2$ for intermediate band materials. *Sol. Energy Mater. Sol. Cells* **144**, 664 (2016).
8. W. Jing, Y. Wang, J. Zhu, W. Yao, and S. Song: Effects of Ti-doping on CuGaS$_2$ thin films by co-sputtering and sulfurizing. *Mater. Lett.* **164**, 513 (2016).
9. N. Armaroli, and V. Balzani: Solar electricity and solar fuels: status and perspectives in the context of the energy transition. *Chem. A Eur. J.* **22**, 32 (2015).
10. X. Lv, S. Yang, M. Li, H. Li, J. Yi, M. Wang, G. Niu, and J. Zhong: Investigation of a novel intermediate band photovoltaic material with wide spectrum solar absorption based on Ti-substituted CuGaS$_2$. *Sol. Energy* **103**, 480 (2014).
11. P. Chen, M. Qin, H. Chen, C. Yang, Y. Wang, and F. Huang: Cr incorporation in CuGaS$_2$ chalcopyrite: a new intermediate-band photovoltaic

material with wide-spectrum solar absorption. *Phys. Stat. Solidi Appl. Mater. Sci.* **210**, 1098 (2013).

12. L. Xiao, J. Zhu, T. Ding, Y. Wang, Y. Fan, and Q. Bo: Synthesis and characterization of Ce-incorporated $CuInS_2$ chalcopyrites. *Mater. Lett.* **159**, 392 (2015).

13. J. Koskelo, J. Hashemi, S. Huotari, and M. Hakala: First-principles analysis of the intermediate band in $CuGa_{1-x}Fe_xS_2$. *Phys. Rev. B* **93**, 165204 (2016).

14. M.M. Han, X.L. Zhang, and Z. Zeng: Sn doping induced intermediate band in $CuGaS_2$. *RSC Adv.* **6**, 110511 (2016).

15. W. Jeong, and G. Park: Structural and electrical properties of CuGaS thin films by electron beam evaporation. *Sol. Energy Mater. Sol. Cells* **75**, 93 (2003).

16. S.K. Kim, J.P. Park, M.K. Kim, K.M. Ok, and I.W. Shim: Preparation of $CuGaS_2$ thin films by two-stage MOCVD method. *Sol. Energy Mater. Sol. Cells* **92**, 1311 (2008).

17. J.A. Hollingsworth, K.K. Banger, M.H.C. Jin, J.D. Harris, J.E. Cowen, E.W. Bohannan, J.A. Switzer, W.E. Buhro, and A.F. Hepp: Single source precursors for fabrication of I-III-VI2 thin-film solar cells via spray CVD. *Thin Solid Films* **431–432**, 63 (2003).

18. S.-H. Chang, B.-C. Chiu, T.-L. Gao, S.-L. Jheng, and H.-Y. Tuan: Selective synthesis of copper gallium sulfide ($CuGaS_2$) nanostructures of different sizes, crystal phases, and morphologies. *CrystEngComm* **16**, 3323 (2014).

19. B. Cordero, V. Gómez, A.E. Platero-Prats, M. Revés, J. Echeverría, E. Cremades, F. Barragán, and S. Alvarez: Covalent radii revisited. *Dalt. Trans.* No. **21**, 2832 (2008).

20. N. Guijarro, M.S. Prevot, X. Yu, X.A. Jeanbourquin, P. Bornoz, W. Bourée, M. Johnson, F. Le Formal, and K. Sivula: A bottom-up approach toward all-solution-processed high-efficiency $Cu(In,Ga)S_2$ photocathodes for solar water splitting. *Adv. Energy Mater.* **6**, 1 (2016).

21. Y. Zhang, Q. Ye, J. Liu, H. Chen, X. He, C. Liao, J. Han, H. Wang, J. Mei, and W. Lau: Earth-abundant and low-cost CZTS solar cell on flexible molybdenum foil. *RSC Adv.* **4**, 23666 (2014).

22. R. Moreno, E.A. Ramirez, and G. Gordillo Guzmán: Study of optical and structural properties of CZTS thin films grown by co-evaporation and spray pyrolysis. *J. Phys. Conf. Ser.* **687**, 012041 (2016).

23. W.P.C. Lee, L.L. Tan, S. Sumathi, and S.P. Chai: Copper-doped flower-like molybdenum disulfide/bismuth sulfide photocatalysts for enhanced solar water splitting. *Int. J. Hydrog. Energy* **43**, 748 (2017).

24. M. Li, R. Zhao, Y. Su, J. Hu, Z. Yang, and Y. Zhang: Synthesis of $CuInS_2$ nanowire arrays via solution transformation of Cu_2S self-template for enhanced photoelectrochemical performance. *Appl. Catal. B Environ.* **203**, 715 (2017).

25. K. Subbaramaiah, and V. S. Raja: Chemical spray deposition of $CuGaS_2$ thin films. *Proc. SPIE* **1523**, 555 (1992).

26. S. Ullah, H. Ullah, F. Bouhjar, M. Mollar, and B. Marí: Synthesis of in-gap band $CuGaS_2$: Cr absorbers and numerical assessment of their performance in solar cells. *Sol. Energy Mater. Sol. Cells* **180**, 322 (2017).

27. R. Strandberg, and I. Aguilera: Evaluation of vanadium substituted In_2S_3 as a material for intermediate band solar cells. *Sol. Energy Mater. Sol. Cells* **98**, 88 (2012).

28. T. Ahsan, S. Kalainathan, N. Miyashita, T. Hoshii, Y. Okada, T. Ahsan, S. Kalainathan, N. Miyashita, T. Hoshii, and Y.O. Characterization: Characterization of Cr doped $CuGaS_2$ thin films synthesized by chemical spray pyrolysis. *Mech. Mater. Sci. Eng. MMSE J. Open Access* **9**, 380 (2017).

29. M. Han, X. Zhang, and Z. Zeng: The investigation of transition metal doped $CuGaS_2$ for promising intermediate band materials. *RSC Adv.* **4**, 62380 (2014).

30. I. Aksenov, Y. Kudo, and K. Sato: Optical absorption spectra in $CuAlS_2$ doped with vanadium. *Jpn. J. Appl. Phys.* **1359**, L145 (1992).